The salmonid and the subsurface: Hillslope storage capacity determines the quality and distribution of fish habitat

D. N. Dralle[1], G. Rossi[2], P. Georgakakos[2], W. J. Hahm[3], D. M. Rempe[4], M. Blanchard[5], M. E. Power[6], W. E. Dietrich[7], and S. M. Carlson[2]

[1] United States Forest Service Pacific Southwest Research Station, Davis, CA, USA
[2] Environmental Science, Policy, and Management, University of California, Berkeley, CA, USA
[3] Department of Geography, Simon Fraser University, Burnaby, BC, Canada
[4] Department of Geological Sciences, University of Texas-Austin, Austin, TX, USA
[5] U.S. Fish and Wildlife Service, Portland, Oregon, USA
[6] Department of Integrative Biology, University of California Berkeley, Berkeley, CA, USA
[7] Department of Earth and Planetary Science, University of California-Berkeley, Berkeley, CA, USA

This paper is a non-peer reviewed preprint submitted to EarthArXiv. It has been submitted to Ecosphere and is under consideration for publication.

The salmonid and the subsurface: Hillslope storage capacity determines the quality and distribution of fish habitat

D. N. Dralle[1], G. Rossi[2], P. Georgakakos[2], W. J. Hahm[3], D. M. Rempe[4], M. Blanchard[5], M. E. Power[6], W. E. Dietrich[7], and S. M. Carlson[2]

[1] United States Forest Service Pacific Southwest Research Station, Davis, CA, USA
[2] Environmental Science, Policy, and Management, University of California, Berkeley, CA, USA
[3] Department of Geography, Simon Fraser University, Burnaby, BC, Canada
[4] Department of Geological Sciences, University of Texas-Austin, Austin, TX, USA
[5] U.S. Fish and Wildlife Service, Portland, Oregon, USA
[6] Department of Integrative Biology, University of California Berkeley, Berkeley, CA, USA
[7] Department of Earth and Planetary Science, University of California-Berkeley, Berkeley, CA, USA

E-mail: `david.dralle@usda.gov`

Open Research statement: Data and code are provided as private-for-peer review via `https://github.com/daviddralle/salmonid_and_subsurface`. Upon acceptance, analysis code and data will be provided via github at `https://github.com/daviddralle/salmonid_and_subsurface`.

Abstract. Water in rivers is delivered via the critical zone that mantles landscapes. Consequently, the success of stream-rearing salmonids depends on the structure and resulting water storage and release processes of this zone. Physical processes below the land surface (the subsurface component of the critical zone) ultimately determine how landscapes 'filter' climate to manifest ecologically significant stream flow and temperature regimes. Subsurface water storage capacity of the critical zone has emerged as a key hydrologic variable that integrates many of these subsurface processes, helping to explain flow regimes and terrestrial plant community composition. Here, we investigate how subsurface storage controls flow, temperature and energetic regimes that matter for salmonids. We illustrate the explanatory power of broadly applicable, storage-based frameworks across a lithological gradient that spans the Eel River watershed of California. Study sites are climatically similar but differ in their geologies and consequent subsurface critical zone structure that dictates water storage dynamics, leading to dramatically different hydrographs, temperature, and riparian regimes – with consequences for every aspect of salmonid life history. Lithological controls on the development of key subsurface critical zone properties like storage capacity suggest a heretofore unexplored link between salmonids and geology, adding to a rich literature that highlights various fluvial and geomorphic influences on salmonid diversity and distribution. Rapidly advancing methods for estimating and observing subsurface water storage dynamics at large scales present new opportunities for more

clearly identifying landscape features that constrain the distributions and abundances of organisms, including salmonids, at watershed scales.

1. Introduction

Riverine biota, including salmonids, depend on multiple facets of streamflow. Flow regime (the timing and magnitude of streamflow) determines the accessibility and hydraulic features of habitat, and influences the timing of key life history events, such as migration and spawning [e.g. Beechie et al., 2006, Sykes et al., 2009]. Stream temperature and riparian light environment impact habitat suitability, fish metabolism, prey productivity, and salmonid growth potential [e.g. Atlas et al., 2021]. Human-caused changes in land use and climate have impacted riverine flows, temperatures, and riparian characteristics, altering aquatic ecosystems globally [Lehner et al., 2011]. Proper attribution of drivers of change, as well as the development of successful mitigation and restoration strategies for aquatic ecosystems, require that we understand the physical controls of these elements at watershed scales [e.g. Sturrock et al., 2019, Quinn et al., 1997].

Although climate strongly influences light environment, temperature, and water quantity and quality [e.g. Berghuijs et al., 2020, Maurer et al., 2021], a full understanding of watershed function requires a critical zone (CZ) perspective, which integrates above-ground processes (e.g., atmospheric fluxes, vegetation patterns, land use changes) with subsurface dynamics (infiltration, rooting zone processes, weathering) and water storage [e.g. Anderson et al., 2007, 2008, Brantley et al., 2007, Riebe et al., 2016, Grant and Dietrich, 2017]. In the upland freshwaters that host many rearing and spawning salmonid populations, water storage in the subsurface CZ occurs in both the shallow soil layer (commonly < 0.5 m thick) and deeper underlying layers of saprolite and weathered bedrock [Rempe and Dietrich, 2018, McCormick et al., 2021, Wald et al., 2013, Dawson et al., 2020].

The dynamic water storage capacity (storage capacity) of the subsurface CZ has emerged as an integrative catchment characteristic because of its ability to explain flowpaths, flow generation, and plant-community composition [Hahm et al., 2019b, Illien et al., 2021, Sayama et al., 2011, McDonnell et al., 2018, Klos et al., 2018]. A watershed's dynamic storage has been defined in various ways [e.g. Staudinger et al., 2017, Dralle et al., 2018, Buttle, 2016], but we here focus on a simple definition of the term: Dynamic storage (ΔS) is the change in volume of water stored in a catchment *relative* to some reference storage state [Hahm et al., 2019b] as inferred through mass balance:

$$\Delta S = P - Q - ET, \tag{1}$$

where P, Q, and ET are precipitation, stream discharge, and evapotranspiration, respectively. In hilly and mountainous landscapes underlain by bedrock, water storage capacity in the subsurface is set by the depth of chemical and physical weathering fronts that alter fresh bedrock and generate porosity capable of retaining and releasing water [e.g. Klos et al., 2018, Pedrazas et al., 2021, Callahan et al., 2020, Holbrook et al., 2014]. These weathering processes, and therefore water storage capacity, depend on tectonics, climate, biota, and, importantly, the underlying bedrock geology [e.g. Riebe et al., 2016]. Exactly determining the water storage capacity of a watershed is intractable, but it can be roughly estimated by simply calculating the maximum observed value of dynamic storage [Hahm et al., 2019b]. Storage capacity in the subsurface sets the maximum volume of water that can be stored for later use by vegetation, which itself interacts with climate and subsurface storage to determine the timing and magnitude of groundwater recharge, and thus runoff generation and river flow regime features [Klos et al., 2018, Dralle et al., 2018].

Here, we propose that subsurface water storage capacity can explain between-catchment differences in stream hydrologic and energetic features that matter for salmonid life history. Importantly, this is not a difference in larger-scale or regional aquifers tied to intrinsic properties of fresh bedrock. Rather, the variability occurs at the hillslope scale and is tied to the weathering-driven development of the critical zone, which depends on material properties of the bedrock. We use California's Eel River—designated by the California Department of Fish and Wildlife and State Water Resources Control Board as a priority salmonid conservation watershed, and one of the few mostly undammed rivers on the US Pacific Coast—as a case study. First, we synthesize results from a decade-plus effort of subsurface monitoring enabled by deep drilling [Salve et al., 2012, Hahm et al., 2020, Schmidt and Rempe, 2020, Tune et al., 2020, Rempe and Dietrich, 2018] showing how subsurface structure and rock type explain variations in water storage capacity and plant community composition at two intensively monitored Eel River subcatchments. These sites are underlain by two different bedrock lithologies (the Coastal Belt turbidites and Central Belt melange of the Franciscan Complex) that have weathered differently (deep and shallow, respectively) owing to different rock properties [Hahm et al., 2019b]. We explore how lithologically-determined storage capacity drives differences in functional features of the flow regime [Yarnell et al., 2020] and energy, and the dynamics and climatic sensitivity of stream temperature between the two subcatchments. We then explore the consequences of these differences for stream rearing salmonids – at specific life stages, and holistically as life history syndromes. Further, we demonstrate in sparsely monitored catchments that estimates of storage capacity explain key metrics of flow behavior, and, across larger watershed scales, storage capacity reflects the contribution from subcatchments of mixed geological composition. Our findings indicate that lithologically controlled storage capacity has widespread impacts on the spatial distribution of habitat quantity and quality, factors that influence the diversity of salmonid life histories.

2. Geology and subsurface structure

The study area encompasses multiple subwatersheds (Table 3 and Figure 2) of the Eel River in the Northern California Coast Ranges. The regional climate is Mediterranean-type with warm, dry summers and cool, wet winters. The Eel River basin is underlain by the Franciscan Complex, a geological assemblage in Northern California consisting of three north-south running belts of different rock type that decrease in age and metamorphic grade from east to west [Blake Jr and Jones, 1974, McLaughlin et al., 1994].

Two intensively monitored watersheds within the Eel River basin, Elder Creek and Dry Creek, serve as representative end members of two (out of three) belts of the Franciscan—the Coastal Belt (Elder Creek) and Central Belt melange (Dry Creek). Figure 1 illustrates lithologically-determined contrasts in hillslope subsurface structure—and thus water storage capacity—in the two watersheds. We here provide a brief overview of the subsurface structures and water storage dynamics at the sites. For more details, we refer the reader to Hahm et al. [2019b].

The Elder Creek watershed is underlain by the fractured shale and sandstones of the Coastal Belt (Figure 1 right column). Deep weathering profiles in the Coastal Belt have resulted in large water storage capacity of the subsurface, most of which is unsaturated storage [Dralle et al., 2018] in a thick vadose zone that includes soil, saprolite, and weathered bedrock. This unsaturated reservoir can hold upwards of 300 mm of seasonally dynamic water storage, equal to more than 1/3 of annual wet season precipitation during dry years [Rempe and Dietrich, 2018]. The large dynamic storage in the vadose zone is the primary water source for the productive, dense conifer-hardwood evergreen forests found in the Coastal Belt. Following the long dry season, tree-driven storage deficits (the amount of water input to the root zone required to replenish that which vegetation removed) in the unsaturated zone are typically replenished within the first few months of the wet season (Oct. to Dec.), whereupon the soil and weathered bedrock layers wet to a characteristic maximum storage. Analogously to 'field capacity' in soils [Grindley, 1968], additional rainfall beyond this characteristic maximum value triggers gravitational drainage that recharges an underlying fractured-rock hillslope groundwater system, which flows laterally down to streams through a system of seeps and springs [Salve et al., 2012, Lovill et al., 2018a]. This deeper saturated reservoir can store upwards of 200 mm of groundwater that slowly drains to adjacent streams, supporting year-round cold baseflows.

Dry Creek is underlain by the Central Belt melange geology (Figure 1 left column), a chaotic mixture of bedrock of varying lithology and size suspended in a shale-derived, clay-rich matrix that is perennially saturated at depths typically not exceeding 2 to 3 m below the ground surface. The thin weathering zone of the Central Belt completely fills after approximately 200 mm of wet season rainfall, at which point the groundwater table rises to the surface, generating widespread saturation overland flow that is rapidly routed to dense drainage networks. Consequently, the Central Belt watersheds are unable to store large volumes of wet season precipitation, resulting in fast draining hillslopes, and streams that cease flowing within the first couple months of the dry season [Lovill et al., 2018a]. Low storage also results in a more water-stress tolerant savanna plant community comprised primarily of Oregon white oak (*Quercus garryana*) and annual grasses [Hahm et al., 2018].

3. Water

Using hydrological and climatic data from the Dry and Elder Creek end members, we explore storage-capacity controls on flow regime features that matter for fish: timing of wet season flow activation (I), peakflow magnitude (II), flow recession rate (III), and low flow magnitude (IV) [Yarnell et al., 2020]. Figure 4 provides an overview of contrasting flow regime features in the end-member Coastal and Central Belt watersheds. Center panels plot discharge on linear (top-central panel) and log (middle-central panel) scales, as well as cumulative discharge and runoff, for the 2019 water year. The paneled subplots aim to highlight the major functional flow components I - IV. Importantly, the sites' 20 km separation results in nearly identical rainstorm magnitudes through the winter.

Conceptual figures illustrate many of these outcomes. A four-quadrant hillslope diagram (Figures 1) depicts representative hydrology for the two end-member geologies in both the wet and dry seasons, and a four-quadrant stream diagram (Figures 3) depicts the typical trajectory of stream conditions from the spring/early summer flow recession to the late-summer low flow period.

3.1. Wet season flow activation

Differences in vegetation cover between Elder and Dry (left versus right column in Figure 1) result in different magnitudes of plant water use, and thus differences in storage deficits in the root zone at the end of the dry season [Dralle et al., 2018, McCormick et al., 2021, Wang-Erlandsson et al., 2016]. Replenishment of these deficits via infiltration of rainfall and filling of the critical zone at the start of the wet season mediates drainage from the root zone, thereby determining the amount of rainfall (more at Elder) required to recharge the hillslope aquifers that drive streamflow production (either via subsurface flow or groundwater-driven saturation overland flow) at the hillslope-channel boundary [Müller et al., 2014, Dralle et al., 2018, Lapides et al., 2021, Grindley, 1968].

To quantify storage controls on wet-season flow activation, we turn to a storage-activation approach introduced by Sayama et al. [2011], wherein early wet season discharge is plotted as a function of cumulative seasonal dynamic watershed storage to identify storage thresholds that lead to rapid increases in discharge. Figure 4I plots stream discharge against a catchment water storage approximation, calculated as the running sum of input (precipitation, P) minus output (discharge, Q) fluxes beginning on October 1, under the assumption that differences between these two dominant fluxes can be attributed to accumulation of storage in the watershed (approximation of Equation 1,

$\Delta S = P - Q - ET \approx P - Q$). Evapotranspiration is neglected because it is expected to be relatively small in October - January when the sum is calculated. Flow activation in Dry Creek begins around approximately 150 mm of cumulative rainfall at the start of the dry season, whereas Elder Creek flow does not activate until approximately 300 mm of rain has fallen. Moreover, Elder Creek discharge sensitivity to storage is much lower, as can be seen by the relatively muted increase in discharge with storage increases beyond 300 mm. The storage-discharge relationship in Dry Creek is more nonlinear ('flashier'), with a very steep increase in flow rate beyond 200 mm of storage.

3.2. Peakflow magnitude

The relationship between storage and discharge also explains the difference in peak flow magnitudes in Figure 4II, where the smaller storage capacity at Dry Creek results in more extreme peak flows. Very small changes in storage generated by the addition of precipitation result in rapid, highly nonlinear increases in flow at Dry Creek, and correspondingly large peak flows, which contrast Elder Creek's muted peak flow response during rainfall events. These flow behaviors can be attributed to water storage dynamics in the hillslope, where complete filling of the critical zone in the Central Belt results in flashy streams fed predominantly by saturation overland flow, as compared to the muted groundwater-dominated signal in Elder Creek, as illustrated in the top row of Figure 1.

3.3. Rate of recession and low (base)flow magnitude

Whereas Figure 4I and II show the effect of storage capacity on rising limb and peakflow behaviors, Figure 4III and IV demonstrate that storage capacity is also a strong determinant of the drainage behavior of the study catchments. At Dry Creek, small storage capacity drives water to the surface, where shallow and overland flowpaths result in fast flow recessions and very little retention of drainable storage. In the Elder Creek watershed, the drainage of deeper fractured rock hillslope groundwater results in a much slower recession and high retention of drainable groundwater storage going into the dry season. The consequences of these recession dynamics are illustrated in the top row of Figure 3. The rapid drop in flows in Central Belt catchments results in relatively mild flow conditions during a short period in the spring (see much of April and May in Figure 4), which contrasts the persistently higher and more turbulent flows during the early dry season in Coastal Belt watersheds.

Over longer periods of drainage—California's protracted dry season can persist for more than six months of the year—storage capacity may dictate whether a stream has any water at all. In our study catchments, two distinct dry season flow regimes emerge: high storage capacity Elder Creek supports robust baseflows that persist through the dry season, whereas ephemeral flows in Dry Creek result in dry streambeds typically before July (Figure 3).

Interestingly, although there is lower *dry season* baseflow in the Dry Creek watershed, over the course of an entire year, Dry Creek typically generates more total runoff for a given precipitation event, as quantified by each watershed's runoff ratio in 4V. From water year 2016 through water year 2020, the average runoff ratio in Elder Creek is approximately 0.6, compared to an average runoff ratio of approximately 0.8 at Dry Creek. The small storage capacity at Dry Creek generates enough runoff during the wet season to overwhelm its small dry season runoff totals, thus producing an overall higher runoff ratio. We attribute this difference primarily to the significant amounts of water stored in the thick weathered bedrock vadose zone at Elder Creek, which results in more water being returned to the atmosphere via transpiration during the growing season.

3.4. Spatial and temporal variability in water availability

In addition to impacting average flow regime features 'at a station', storage capacity can also mediate the spatial availability of water via the wetted channel network, and the sensitivity of runoff dynamics to year-to-year swings in rainfall totals. For example, Lovill et al. [2018a] demonstrate significant differences in wetted channel drainage density between the Elder Creek and Dry Creek watersheds. Figure 5 reproduces results from Lovill et al. [2018a], plotting a snapshot of wetted channel extent in late August 2014. On this date, Elder Creek wetted channel drainage density is nearly 10 times greater than that observed in Dry Creek, despite nearly identical rainfall totals in the preceding wet season.

Regarding temporal variability in water availability, Hahm et al. [2019a] introduce the idea that *small* subsurface water storage capacity *relative* to annual average rainfall has the potential to decouple initial storage going into the summer (which sets plant water availability during the dry growing season) from total annual rainfall. This mechanism was dubbed 'storage-capacity limitation', wherein the limited subsurface water storage capacity fills completely in both wet and dry years, resulting in a hydrological mechanism of drought resilience. Although Hahm et al. [2019a] explore this concept with respect to vegetation response to annual rainfall variability, it extends to components of hydrograph variability as well. Specifically, since storage-controlled flow conditions going into the dry season control summer low flows [Dralle et al., 2016], if storage is decoupled from *total* rainfall, so too will be low flows. In both Elder Creek and Dry Creek, we find that dry season low flows are essentially decoupled from annual swings in total rainfall (both are storage-capacity limited). This is because storage capacity in both watersheds is significantly lower than average annual precipitation, and therefore annual variations in total rainfall do not lead to annual variations in dynamic storage going into the dry season, resulting in a decoupling of low flows from total rainfall. In the case of Dry Creek, this decoupling result is trivial; low flows are reliably zero in all years, and therefore total annual rainfall does not dictate low flow magnitudes. At Elder Creek, Figure 8a illustrates how dry season initial flow conditions and dry season duration are likely more important drivers of low flows (not total annual rainfall). Figure 8b quantifies the decoupling between low flow and annual rainfall, demonstrating that low flow magnitude (over 21 years, 2001 to 2021) does not vary strongly with total rainfall. Consistent with the storage-capacity limitation mechanism hypothesized by Hahm et al. [2019a], a linear regression reveals no significant slope on the low flow vs. water year precipitation relationship, with an R^2 of 0.14, indicating that water year precipitation explains little of the variation in summer low flows.

3.5. Hydrological scaling in mixed-lithology watersheds

Large watersheds can be conceived of as a collection of hillslopes connected through a shared channel network [Harman et al., 2009]. Using this "unit hillslope" concept, and under the assumption that a map of Coastal and Central Belt geologies may serve as a proxy for hillslope storage capacity across the Eel River, we hypothesize that "mixed lithology" watersheds will behave, hydrologically, like a superposition of the Elder Creek and Dry Creek geological end members. To test this hypothesis, we identified 5 subwatersheds (Table 3) of the Eel River with contributing areas less than 1000 km^2 that span a gradient in percent melange composition, where Dry Creek serves as the 100% melange watershed, and Elder Creek serves as the 0% melange watershed. We explore scaling of flow recession and dry season water availability across this geological spectrum of sites.

We perform two analyses to explore drivers of the scaling of dry season flow recession and water availability in the watersheds listed in Table 3. First, we calculated a dimensionless metric of summer water availability, the summer runoff fraction, which is calculated as the long term average of the annual ratio of total flow from June through September (summer dry season) divided by total flow from the previous October through May (preceding wet season). Second, we calculated the average flow recession rate using the widely used exponential flow recession model:

$$\frac{dQ}{dt} = -\frac{1}{\tau}Q \quad \rightarrow \quad Q = Q_0 e^{-t/\tau},$$

where Q_0 is the initial flow value at the start of the recession. The recession timescale, τ (with units of time), is a scale-independent measure of the rate of recession and is therefore directly comparable between watersheds of different sizes and with different average flow values.

Watersheds with greater percent Central Belt mélange contributing area have less summer runoff relative to annual total runoff (Figure 6c). At Elder Creek (0% mélange), we see an average 3.75% of annual runoff discharges during the summer months. There is a monotonic decrease in summer runoff fraction, with effectively 0% of annual runoff occurring during the summer months in Dry Creek (100% mélange).

Figure 6a,b show why summer runoff fractions are so small in mélange-dominated watersheds: typical flow recession rates, as quantified by the linear recession timescale (τ) decrease nearly ten-fold across the geological gradient, from approximately $\tau = 10$

days at Elder Creek, to $\tau = 1$ day at Dry Creek. Actual recession data in Figure 6a demonstrates how smaller recession τ results in a more rapid drop in flows in watersheds with higher mélange fraction.

4. Energy

Different subsurface water storage capacities support distinct vegetation types: dense, shady forest at Elder Creek, and at Dry Creek a deciduous oak savanna admitting more solar radiation (Figure 3. Differences in runoff pathways and flow volumes between the Elder Creek and Dry Creek watersheds should also affect stream temperature and its sensitivity to changes in atmospheric conditions. Deeper groundwater flowpaths in Coastal Belt geologies (Figure 1) are more buffered from variations in air temperature. The thermal inertia of a stream can also be expected to vary with flow volumes; all else equal, stream temperature will be more responsive to changing air temperature at smaller flow volumes. For all these reasons, stream temperature in watersheds with lower storage capacity, like Dry Creek, should track changes in air temperature more closely.

4.1. Channel shading

Large differences in canopy cover between the two geologies can be seen in Figure 7a. These storage-driven differences in vegetation community and canopy cover affect the riparian light environment. To quantify this, we calculated a simplified light penetration index (LPI) metric [Bode et al., 2014] as the number of LiDAR point returns that strike either ground or water divided by the total number of LiDAR returns at a 1 m resolution across all available LiDAR datasets in the Eel River [Power, 2013, Dietrich, 2014, Roering, 2006, Perkins, 2009, Dietrich, 2015]. The LPI estimates the fraction of shortwave radiation that penetrates the vegetation canopy to reach the ground or water surface. Using mapped LPI, we computed reach-averaged canopy closure (Figure 7b) throughout the Eel River basin, illustrating a significant shift in stream shading across the Coastal and Central Belt lithologic contact. We then explored how this shift in riparian cover impacts the growing season stream energy budget by first extracting total summer shortwave solar radiation delivery (June through August) the midpoint (latitude 39.64, longitude -123.53) of the centroids of the Elder and Dry Creek watersheds [Thornton et al., 2020], then multiplying this figure by reach-averaged LPI to arrive at an estimate of total shortwave solar energy delivery to streams over the peak growing season months.

Figure 7c plots the reach-scale, LPI-filtered solar shortwave radiation energy delivery across a range of watershed contributing areas for the two lithologies. At small contributing areas, solar energy delivery to the channel is nearly three times greater in Central Belt versus Coastal Belt watersheds. However, as contributing area increases, channel widths tend to increase, leading to an overall increase in solar radiation delivery and a convergence between the two lithologies: streamside vegetation shading matters less in wide channels.

4.2. Stream temperature

Figure 7d plots air temperature and stream temperature at the end-member sites, clearly demonstrating that Dry Creek water temperatures fluctuate more widely than those in Elder Creek despite nearly identical air temperatures between the two sites. Figure 7e removes the time element to reveal the relationship between water temperature and air temperature. Best fit lines between Elder Creek and Dry Creek show that water temperature is generally buffered relative to air temperature as expected from its higher heat capacity (slope less than 1) but that Dry Creek's best fit line slope is nearly double that of Elder Creek, indicating that Dry Creek water temperature is much more sensitive to air temperature changes.

5. Discussion

5.1. Salmonids and the Subsurface - Life history framework and hypotheses

Properties of the subsurface critical zone have consequences for salmonids across every stage of their life history. Environmental regimes determined by a watershed's storage capacity in turn constrain (Table 2) opportunities for salmon, influencing access for migrating and spawning adults, the survival of eggs, and the rearing habitats and movements of juveniles during their freshwater residence. Below we delve deeper into these connections and consider how watershed storage capacity influences core events in the life history of salmonids, using Elder Creek and Dry Creek as representative ecological end-members. In particular, we emphasize that contrasting conditions that favor different life history traits. Further, we suggest that the watershed behaviors of Elder and Dry Creek, driven by their distinct subsurface storage capacities, could select for life history syndromes, that is, suites of correlated traits (e.g. spawn timing, growth and foraging, and movement decisions), associated with different degrees of dependence on rearing in natal habitat (i.e., habitat in which they emerged) versus rearing outside their natal habitat (i.e., non-natal rearing). Life history variation among populations in contrasting CZ environments could reflect natural selection (i.e., life history adaptation) or plasticity. Regardless, we posit the habitat conditions in different CZ environments tend to favor expression of different (and specific) life histories.

5.1.1. Adult migration and spawning Migration and spawning require suitable depth of flow for passage between the ocean and riverine spawning sites and suitable hydraulics for spawning once fish arrive at their spawning destination. The site-specific lag time between a rainfall event and the hydraulic response in streams determines how quickly migrating and spawning salmon can respond to precipitation. Subsurface storage deficits at the end of the dry season dictate how much precipitation is needed to elevate winter stream flows in the early wet season [Rempe and Dietrich, 2018, Dralle et al., 2018]. For example, when root-zone storage is fully depleted, flow activation requires twice as much precipitation in Elder Creek as in Dry Creek. Thus, in low-storage capacity watersheds like Dry Creek, less precipitation is needed to provide suitable flows for migration and spawning, potentially allowing spawning to occur earlier in these systems. In higher storage capacity systems like Elder Creek, a later wet season flow activation, but more prolonged flow recession, suggests adults may arrive and spawn later – but enjoy a longer duration of suitable spawning conditions. The difference in flow activation between Elder and Dry Creek may vary from hours to weeks depending on their respective storage capacity deficits and initial wet season rainfall patterns. Variation in subsurface storage capacity, therefore, is likely to generate differences in access and spawn timing during many years, similar to the influence of stream temperature in influencing diversity in this trait among populations [e.g. Lisi et al., 2013].

5.1.2. Egg incubation Female salmon build their redds (nests) in the gravel of streambeds. The shape of the redd, the location, and the size of the gravels all differ among species. The developmental rate of eggs also differs among species and is strongly influenced by water temperature [From and Rasmussen, 1991]. Temperature variation among streams driven by subsurface properties (see Figure 7), and contributions to discharge from ground water, likely have consequences for egg development rates and fry emergence timing. Riparian vegetation composition and flow volume (thermal mass)– both controlled by features of the Critical Zone–affect the sensitivity of stream water temperature to air temperature and solar radiation (Figure 7). Ephemeral Dry Creek, with its minimal channel shading, warms (and cools) more rapidly than heavily shaded Coastal Belt streams with sustained contributions from groundwater, like Elder Creek. Eggs incubating in redds in the warmer waters of intermittent streams are likely to develop more rapidly, leading to earlier alevin emergence.

In addition to the effect of temperature on egg emergence, salmon redds are at risk of scour and dessication depending, in part, on the flashiness of stream hydrology [Orth et al., 2005]. Rapid declines in streamflow can potentially cause redds to dry before alevin are able to emerge. Conversely higher peak flows lead to greater risk of redd scour. In short, in flashy melange streams like Dry Creek, redds are likely also more at risk from scour and desiccation than in more stable streams with lower peak flows like Elder Creek (Figure 3).

5.1.3. Juvenile growth and summer survival Once salmon fry have emerged from the gravels and begin exogenous feeding, differences in CZ structure have implications for the prey production and growth of fish during their early life stages. During the spring months (March-May), streamflow recession coincides with increasing photo-period and primary and secondary productivity in salmon-bearing food webs of coastal streams like Elder and Dry Creek [Rossi et al., 2022]. However, the relative timing and rate of streamflow recession, water temperature warming, and food web phenology all vary between stream types (Figure 6), driving different seasonal patterns in growth potential for rearing salmonids [Rossi et al., 2022]. All else being equal, streams fed by Critical Zones with low storage capacity will support an earlier spring increase in juvenile salmonid growth potential, and an earlier decrease in summer growth potential; whereas in perennial streams fed by Critical Zones with high storage, growth potential for juvenile salmonids will peak later and be sustained longer [Rossi et al., 2022].

While growth potential may peak earlier in intermittent streams with low storage potential, these systems also experience an earlier onset of inhospitable conditions for summer rearing salmonids. With warming and hypoxia, and eventual drying and disconnection of the wetted channel network, fish that remain in the stream (as opposed to outmigrating, see next section) can perish [Rossi et al., 2022, Labbe and Fausch, 2000]. Importantly, the magnitude of summer mortality varies considerably among years due to interannual variation in rainfall patterns [Hwan et al., 2018, Obedzinski et al., 2018]. Recent work by Vander Vorste et al. [2020], however, highlights that some intermittent systems provide more reliable habitats for juvenile coho rearing. For example, across the geologically complex Russian River watershed in Sonoma County, California, inter-annual variation in summer survival was high at some sites, but much more stable at other sites, hinting at the importance of CZ properties in influencing sensitivity of different systems to inter-annual variation in rainfall and consequences for salmon survival (e.g. Figure 6; see also Moidu et al. [2021]).

5.1.4. Life history syndromes A particularly diverse component of the many life histories of anadromous salmonids [Shapovalov and Taft, 1954, Hodge et al., 2016] is residence time of juveniles in their natal streams and their corresponding dependence, or lack thereof, on rearing outside their natal habitats. Here we suggest that watersheds with different and distinct subsurface storage capacities will favor the emergence of life history syndromes, that is, suites of correlated traits associated with different degrees of dependence on natal and non-natal rearing.

In non-perennial systems such as Dry Creek, faster recession that lowers summer base flow should favor a "grow fast and outmigrate early in life" strategy [e.g. Erman and Leidy, 1975], while earlier flow activation will allow adults to access and spawn sooner than in perennial streams (Figure 3). Warmer water would also directly accelerate egg development in non-perennial streams (Figure 7), so both earlier spawn timing and faster incubation should result in earlier emergence of juveniles. Earlier increases in food availability in sunlit channels support an earlier spring peak in growth potential in intermittent versus perennial streams [Rossi et al., 2022, Ebersole et al., 2006]. When the wetted channel dries completely or conditions become lethal, however, outmigration before the stream dries is the only option for survival. Erman and Leidy [1975] reported that large numbers of *O. mykiss* fry outmigrated from an intermittent stream prior to stream drying, suggesting that these systems contribute to diversity of outmigration timing. In the second year of their study, with more precipitation and perennial summer flows, many juveniles over-summered in the tributary, highlighting the influence of interannual variation in precipitation on life history expression. Over-summering salmonids have also been regularly observed in intermittent streams with remnant pools with adequate water quality that persists through the summer [e.g. Obedzinski et al., 2018, Hwan et al., 2018, Woelfle-Erskine et al., 2017, Grantham et al., 2012, Vander Vorste et al., 2020]. However, wetted habitat area in such channels can be extremely limited, particularly habitats where older (i.e., age 1+ and 2+) fish can rear. In short, these streams can produce large numbers of outmigrating juveniles, but the success of this strategy relies on non-natal growth opportunities elsewhere in the watershed.

In contrast, in perennial streams with year-round flow, more critical zone storage of precipitation delays runoff pulses that allow adults to access spawning locations, delaying spawn timing (Figure 4), while cooling groundwater inputs during the spring as eggs incubate (Figure 7) slow development of incubating eggs, delaying emergence relative to the timing of these events in non-perennial streams. However, the slower rate of flow recession in spring and higher mean summer base flows can support fish that over-summer in the stream and rear for at least one year before outmigration [Kelson and Carlson, 2019]. Secondary production increases later than in intermittent streams, which along with sustained recessions and greater channel shading, leads to a later peak in growth potential [Rossi, 2020]. Perennial flow creates a greater extent of wetted channel and sustained summer rearing environment (both space and water quality), and reduces summer mortality relative to intermittent streams.

5.2. Storage capacity's influence on stream energetics

We identified three mechanisms by which hillslope storage dynamics could impact stream temperature and light environment. First, storage-controlled plant community composition has consequences for stream shading. Second, flow volumes impact the thermal inertia of water in the channel; all else being equal, lower flows in low storage Dry Creek result in higher in-channel sensitivity of water temperature to radiation fluxes and air temperature [Webb et al., 2008]. Finally, storage dictates flowpaths to streams, and because near-surface versus deep flowpaths will have different sensitivities to air temperature, this ultimately will impact the temperature of groundwater and water delivery to channels [Kurylyk et al., 2015]. We found water temperature dynamics were consistent with all three of these mechanisms; specifically, the low storage Dry Creek catchment has flow temperatures that are both hotter and more sensitive to climate than the high storage capacity Elder Creek catchment during the warm summer months. Although we did not determine the relative strengths of these three mechanisms, we did demonstrate potential scale-dependence in their impacts. At large scales, channels are wide and therefore hillslope plant communities have less impact on shading. At small scales (headwaters), water has not resided in channel for long and in-stream temperatures may be more representative of water temperatures being delivered to the channel by the hillslope [Dugdale et al., 2017]. Although there have been exciting advances toward incorporating the impacts of flowpaths and hillslope processes in stream temperature prediction [Leach and Moore, 2015, Hrachowitz et al., 2010], most efforts focus on climate factors or heat exchange at the stream surface or with channel substrate [Brown, 1969]. Increased focus on hillslope processes will be especially important for understanding the fate of headwater refugia during low flow periods [Isaak et al., 2016, Leach and Moore, 2017], where prediction of water temperature sensitivities to climate are highly dependent hillslope processes [e.g. groundwater flow Leach and Moore, 2019] and properties [e.g. depth to bedrock Briggs et al., 2018].

5.3. Measuring and modeling storage capacity

Storage capacity has predictive potential for ecology, yet is difficult to measure or estimate; the *in situ* methods deployed at Dry Creek and Elder Creek cannot be realistically deployed at larger scales relevant to managers. Geological maps can be used to extrapolate behaviors over larger scales (under the assumption that rock-type is the primary driver of hillslope weathering profiles), but inferences need to be grounded with data from intensively monitored sites. Alternative approaches to analyzing storage in environments where data are sparse have emerged in recent years . Where discharge data are available, storage-discharge methods and models, or dynamic storage tracking, can provide important insights into subsurface storage processes and their controls on hydrology [Sayama et al., 2011] and salmonid-relevant flow metrics [Soulsby et al., 2016]. Satellite remote sensing methods have emerged as a scaleable approach for monitoring plant-driven storage deficits [Wang-Erlandsson et al., 2016], which control flow activation. Maximum observed storage deficits have been correlated with storage capacity as well [McCormick et al., 2021, Stocker et al., 2021]. Geomorphological, ecological, and hydrological model inversion and inferential methods may also provide some insights into the thickness of weathering profiles and water storage capacity [Pelletier et al., 2016, Ichii et al., 2009, Kleidon, 2004, Schenk, 2008]. Finally, geophysical methods, such as seismic refraction, have shown promise for understanding ecologically important hillslope-scale storage dynamics with significantly less effort than invasive methods [Holbrook et al., 2014, Briggs et al., 2018].

5.4. The evolution of hillslopes and salmon

Geologic history [e.g. Waples et al., 2008], landscape evolution [e.g. Montgomery, 2000] and channel network dynamics [e.g. Stokes and Perron, 2020, Val et al., 2022], and, on the shorter time scales, erosional and flood dynamics [Waples et al., 2008], all influence salmon diversity and resilience in the Anthropocene. Here we add another geomorphic component: the critical zone. The evolution of *subsurface* hillslope critical zone properties—including subsurface water storage capacity—depend on complex interactions between hydrology, weathering, erosion and tectonics [Riebe et al., 2016]. We highlighted the dependence of storage capacity on rock properties, but other work demonstrates how subsurface architecture may also be influenced by frost cracking, regional tectonic stresses, and groundwater geochemistry [Riebe et al., 2016, Rempe and Dietrich, 2014, St. Clair et al., 2015, Brantley and Lebedeva, 2011, Anderson et al., 2013, Harman and Kim, 2019]. Watershed hydrologic behavior arises from the collected dynamics of individual hillslopes, whose subsurface capacity to transmit flow downslope dictates the spatial extent of runoff generation. Over longer timescales, runoff drives the erosion of channels and the evolution of river networks [Beven and Kirkby, 1979, Litwin et al., 2020, Deal et al., 2018], the properties of which have direct consequences for the extent of wetted channel [Prancevic and Kirchner, 2019, Moidu et al., 2021] and aquatic habitat [Hwan and Carlson, 2016, Sabo et al., 2010]. Additional lithologically influenced hillslope and channel processes that impact habitat include base-level change induced propagation of knickpoints up channel networks as well as the introduction of static knickpoints in the form of megaboulders [Roering et al., 2015, Bennett et al., 2016], both of which occur in the Eel River watershed and can act as barriers to fish passage. Longer-term geologic and tectonic processes have been used to explain aspects of salmonid evolution, spatial distribution, and life-history strategies [Montgomery, 2000, Montgomery et al., 2003, Hassan et al., 2008, Waples et al., 2008], but the potential indirect effects of these processes on salmonids via the formation of hillslopes, patterns of subsurface storage, and the genesis river flow-temperature regimes have not been previously identified.

We build on earlier research to emphasize that subsurface critical zone diversity likely favors expression of distinct salmonid life histories, and may lead to the emergence of life history syndromes. These include fry dispersing from ephemeral streams early in life and rearing downstream in non-natal habitats prior to ocean entry [Everest et al., 1973], fish over-summering in intermittent streams with refuge pools and out-migrating the following year [e.g. Hwan et al., 2018], and perennial streams supporting juveniles for one to two years prior to out-migration and, in the case of *O. mykiss*, trout completing the entire life history in the stream (as resident rainbow trout) [e.g. Kelson et al., 2020]. Thus, different critical zones within a watershed create a mosaic of habitats with different seasonalities and channel characteristics, which likely favor and support distinct life histories.

The success of different life histories will also vary across years due to variation in flow activation and access to tributary breeding habitats, potential for redd scour, spring flow recession and channel warming dynamics, connectivity to downstream non-natal rearing habitat, and disconnectivity of habitats and exposure to lethal temperatures – all of which are consequences of how climate is filtered through the critical zone. Across the watershed, maintaining a suite of salmonid populations that differ in their life histories may generate a portfolio effect, wherein the complex of populations is more stable than the individual populations [Schindler et al., 2010]. This suggests that the geography of critical zone structure may be an important factor contributing to the stability of salmonid population complexes, and that mapping the diversity of critical zones across the watershed may be essential to developing successful strategies for sustaining salmon in an era of change.

6. Conclusion

A lithological gradient across California's Eel River illustrates the power of broadly applicable, storage-based frameworks to explain energetic and flow features of the stream environment that directly affect behavior and growth of riverine biota, such as salmonids. Different critical zones create a mosaic of habitats that likely favor and support different salmonid life histories, and may contribute to a stabilizing portfolio effect. Looking beyond the Eel River, our work motivates deeper study of geological and landscape controls on subsurface water storage capacity. At present, subsurface water supply is poorly mapped beyond shallow soils, despite increasing recognition that storage in deeper layers of weathered bedrock plays an essential role in determining moisture availability and runoff production in water-limited environments. Rapidly advancing methods for estimating and observing subsurface water storage dynamics at large scales present new opportunities for more clearly identifying landscape factors that influence aquatic biota. The linkages between water storage capacity, flow regime, stream energetics, and their consequences for salmonid life history expression highlight the need for a subsurface perspective on how landscapes and their evolution influence salmonid fishes. Better understanding the consequences of different critical zones for salmon life history diversity would help managers support resilient salmon populations.

Data and code availability

All plotting and analysis codes, and data used to generate plots, are available through Google Colaboratory Python notebooks posted on GitHub at `https://github.com/daviddralle/salmonid_and_subsurface`.

Acknowledgements

LiDAR-derived LPI analysis based on services provided by NCALM through the OpenTopography Facility with support from the National Science Foundation under NSF Award Numbers 1948997, 1948994 and 1948857. We acknowledge support from the National Science Foundation CZP EAR-1331940 for the Eel River Critical Zone Observatory. We thank C. Bode for sensor and data assistance.

References

Robert S Anderson, Suzanne P Anderson, and Gregory E Tucker. Rock damage and regolith transport by frost: An example of climate modulation of the geomorphology of the critical zone. *Earth Surface Processes and Landforms*, 38(3):299–316, 2013.

Suzanne Prestrud Anderson, Friedhelm von Blanckenburg, and Arthur F White. Physical and chemical controls on the critical zone. *Elements*, 3(5):315–319, 2007.

Suzanne Prestrud Anderson, Roger C Bales, and Christopher J Duffy. Critical zone observatories: Building a network to advance interdisciplinary study of earth surface processes. *Mineralogical Magazine*, 72(1):7–10, 2008.

William I. Atlas, Karl M. Seitz, Jeremy W.N. Jorgenson, Ben Millard-Martin, William G. Housty, Daniel Ramos-Espinoza, Nicholas J. Burnett, Mike Reid, and Jonathan W. Moore. Thermal sensitivity and flow-mediated migratory delays drive climate risk for coastal sockeye salmon. *FACETS*, 6(1):71–89, Jan 2021. ISSN 2371-1671. doi: 10.1139/facets-2020-0027. URL `http://dx.doi.org/10.1139/facets-2020-0027`.

Timothy Beechie, Eric Buhle, Mary Ruckelshaus, Aimee Fullerton, and Lisa Holsinger. Hydrologic regime and the conservation of salmon life history diversity. *Biological Conservation*, 130(4):560–572, Jul 2006. ISSN 0006-3207. doi: 10.1016/j.biocon.2006.01.019. URL `http://dx.doi.org/10.1016/j.biocon.2006.01.019`.

Georgina L Bennett, Scott R Miller, Joshua J Roering, and David A Schmidt. Landslides, threshold slopes, and the survival of relict terrain in the wake of the mendocino triple junction. *Geology*, 44(5):363–366, 2016.

Wouter R Berghuijs, Sebastian J Gnann, and Ross A Woods. Unanswered questions on the budyko framework. *Hydrological Processes*, 34(26):5699–5703, 2020.

Keith J Beven and Michael J Kirkby. A physically based, variable contributing area model of basin hydrology/un modèle à base physique de zone d'appel variable de l'hydrologie du bassin versant. *Hydrological sciences journal*, 24(1):43–69, 1979.

M Clark Blake Jr and David L Jones. Origin of franciscan melanges in northern california. 1974.

Collin A. Bode, Michael P. Limm, Mary E. Power, and Jacques C. Finlay. Subcanopy solar radiation model: Predicting solar radiation across a heavily vegetated landscape using lidar and gis solar radiation models. *Remote Sensing of Environment*, 154: 387–397, Nov 2014. ISSN 0034-4257. doi: 10.1016/j.rse.2014.01.028. URL `http://dx.doi.org/10.1016/j.rse.2014.01.028`.

Susan L Brantley and Marina Lebedeva. Learning to read the chemistry of regolith to understand the critical zone. *Annual Review of Earth and Planetary Sciences*, 39: 387–416, 2011.

Susan L Brantley, Martin B Goldhaber, and K Vala Ragnarsdottir. Crossing disciplines and scales to understand the critical zone. *Elements*, 3(5):307–314, 2007.

Martin A Briggs, John W Lane, Craig D Snyder, Eric A White, Zachary C Johnson, David L Nelms, and Nathaniel P Hitt. Shallow bedrock limits groundwater seepage-based headwater climate refugia. *Limnologica*, 68:142–156, 2018.

George W Brown. Predicting temperatures of small streams. *Water resources research*, 5(1):68–75, 1969.

James M. Buttle. Dynamic storage: a potential metric of inter-basin differences in storage properties. *Hydrological Processes*, 30(24):4644–4653, Jul 2016. ISSN 0885-6087. doi: 10.1002/hyp.10931. URL `http://dx.doi.org/10.1002/hyp.10931`.

Russell P. Callahan, Clifford S. Riebe, Sylvain Pasquet, Ken L. Ferrier, Dario Grana, Leonard S. Sklar, Nicholas J. Taylor, Brady A. Flinchum, Jorden L. Hayes, Bradley J. Carr, and et al. Subsurface weathering revealed in hillslope-integrated porosity distributions. *Geophysical Research Letters*, 47(15), Aug 2020. ISSN 1944-8007. doi: 10.1029/2020gl088322. URL `http://dx.doi.org/10.1029/2020GL088322`.

Todd E Dawson, W Jesse Hahm, and Kelsey Crutchfield-Peters. Digging deeper: what the critical zone perspective adds to the study of plant ecophysiology. *New Phytologist*, 226(3):666–671, 2020.

Eric Deal, Jean Braun, and Gianluca Botter. Understanding the role of rainfall and hydrology in determining fluvial erosion efficiency. *Journal of Geophysical Research: Earth Surface*, 123(4):744–778, 2018.

William E. Dietrich. Eel River Critical Zone Observatory July 2014 Lidar Survey. 2014. doi: 10.5069/G9WH2N2P.

William E. Dietrich. Laytonville, CA LiDAR 2015 Airborne LiDAR Survey. 2015. doi: 10.5069/G9WH2N2P.

David N Dralle, Nathaniel J Karst, and Sally E Thompson. Dry season streamflow persistence in seasonal climates. *Water Resources Research*, 52(1):90–107, 2016.

David N. Dralle, W. Jesse Hahm, Daniella M. Rempe, Nathaniel J. Karst, Sally E. Thompson, and William E. Dietrich. Quantification of the seasonal hillslope water storage that does not drive streamflow. *Hydrological Processes*, 32(13):1978–1992, May 2018. ISSN 0885-6087. doi: 10.1002/hyp.11627. URL `http://dx.doi.org/10.1002/hyp.11627`.

Stephen J Dugdale, David M Hannah, and Iain A Malcolm. River temperature modelling: A review of process-based approaches and future directions. *Earth-Science Reviews*, 175:97–113, 2017.

Joseph L Ebersole, Parker J Wigington Jr, Joan P Baker, Michael A Cairns, M Robbins Church, Bruce P Hansen, Bruce A Miller, Henry R LaVigne, Jana E Compton, and Scott G Leibowitz. Juvenile coho salmon growth and survival across stream network seasonal habitats. *Transactions of the American Fisheries Society*, 135(6):1681–1697, 2006.

Don C Erman and George R Leidy. Downstream movement of rainbow trout fry in a tributary sagehen creek, under permanent and intermittent flow. *Transactions of the American Fisheries Society*, 104(3):467–473, 1975.

Fred H Everest, Oregon State Game Commission, et al. Ecology and management of summer steelhead in the rogue river. 1973.

Jon From and Gorm Rasmussen. Growth of rainbow trout, oncorhynchus mykiss (walbaum, 1792) related to egg size and temperature. *Dana*, 9:31–38, 1991.

Gordon E Grant and William E Dietrich. The frontier beneath our feet. *Water Resources Research*, 53(4):2605–2609, 2017.

Theodore E Grantham, David A Newburn, Michael A McCarthy, and Adina M Merenlender. The role of streamflow and land use in limiting oversummer survival of juvenile steelhead in california streams. *Transactions of the American Fisheries Society*, 141(3):585–598, 2012.

J Grindley. The estimation of soil moisture deficits. *Water for Peace: Water supply technology*, 3:241, 1968.

W. J. Hahm, D. N. Dralle, D. M. Rempe, A. B. Bryk, S. E. Thompson, T. E. Dawson, and W. E. Dietrich. Low subsurface water storage capacity relative to annual rainfall decouples mediterranean plant productivity and water use from rainfall variability. *Geophysical Research Letters*, 46(12):6544–6553, Jun 2019a. ISSN 1944-8007. doi: 10.1029/2019gl083294. URL `http://dx.doi.org/10.1029/2019GL083294`.

W. Jesse Hahm, William E. Dietrich, and Todd E. Dawson. Controls on the distribution and resilience ofquercus garryana: ecophysiological evidence of oak's water-limitation tolerance. *Ecosphere*, 9(5):e02218, May 2018. ISSN 2150-8925. doi: 10.1002/ecs2.2218. URL `http://dx.doi.org/10.1002/ecs2.2218`.

W Jesse Hahm, Daniella M Rempe, David N Dralle, Todd E Dawson, Sky M Lovill, Alexander B Bryk, David L Bish, Juergen Schieber, and William E Dietrich. Lithologically controlled subsurface critical zone thickness and water storage capacity determine regional plant community composition. *Water Resources Research*, 55(4): 3028–3055, 2019b.

WJ Hahm, DM Rempe, DN Dralle, TE Dawson, and WE Dietrich. Oak transpiration drawn from the weathered bedrock vadose zone in the summer dry season. *Water Resources Research*, 56(11):e2020WR027419, 2020.

C. J. Harman, M. Sivapalan, and P. Kumar. Power law catchment-scale recessions arising from heterogeneous linear small-scale dynamics. *Water Resources Research*, 45(9), Sep 2009. ISSN 0043-1397. doi: 10.1029/2008wr007392. URL `http://dx.doi.org/10.1029/2008WR007392`.

Ciaran J Harman and Minseok Kim. A low-dimensional model of bedrock weathering and lateral flow coevolution in hillslopes: 1. hydraulic theory of reactive transport. *Hydrological processes*, 33(4):466–475, 2019.

Marwan A Hassan, Allen S Gottesfeld, David R Montgomery, Jon F Tunnicliffe, Garry KC Clarke, Graeme Wynn, Hale Jones-Cox, Ronald Poirier, Erland MacIsaac, Herb Herunter, et al. Salmon-driven bed load transport and bed morphology in mountain streams. *Geophysical research letters*, 35(4), 2008.

Brian W Hodge, Margaret A Wilzbach, Walter G Duffy, Rebecca M Quiñones, and James A Hobbs. Life history diversity in klamath river steelhead. *Transactions of the American Fisheries Society*, 145(2):227–238, 2016.

W. Steven Holbrook, Clifford S. Riebe, Mehrez Elwaseif, Jorden L. Hayes, Kyle Basler-Reeder, Dennis L. Harry, Armen Malazian, Anthony Dosseto, Peter C. Hartsough, and Jan W. Hopmans. Geophysical constraints on deep weathering and water storage potential in the southern sierra critical zone observatory. *Earth Surface Processes and Landforms*, 39(3):366–380, Jan 2014. doi: 10.1002/esp.3502.

Markus Hrachowitz, Chris Soulsby, Christian Imholt, IA Malcolm, and Doerthe Tetzlaff. Thermal regimes in a large upland salmon river: a simple model to identify the influence of landscape controls and climate change on maximum temperatures. *Hydrological Processes*, 24(23):3374–3391, 2010.

Jason L Hwan, Albert Fernández-Chacón, Mathieu Buoro, and Stephanie M Carlson. Dry season survival of juvenile salmonids in an intermittent coastal stream. *Canadian Journal of Fisheries and Aquatic Sciences*, 75(5):746–758, 2018.

JL Hwan and SM Carlson. Fragmentation of an intermittent stream during seasonal drought: Intra-annual and interannual patterns and biological consequences. *River Research and Applications*, 32(5):856–870, 2016.

Kazuhito Ichii, Weile Wang, Hirofumi Hashimoto, Feihua Yang, Petr Votava, Andrew R Michaelis, and Ramakrishna R Nemani. Refinement of rooting depths using satellite-based evapotranspiration seasonality for ecosystem modeling in california. *Agricultural and Forest Meteorology*, 149(11):1907–1918, 2009.

L. Illien, C. Andermann, C. Sens-Schönfelder, K. L. Cook, K. P. Baidya, L. B. Adhikari, and N. Hovius. Subsurface moisture regulates himalayan groundwater storage and discharge. *AGU Advances*, 2(2), May 2021. ISSN 2576-604X. doi: 10.1029/2021av000398. URL `http://dx.doi.org/10.1029/2021AV000398`.

Daniel J Isaak, Michael K Young, Charles H Luce, Steven W Hostetler, Seth J Wenger, Erin E Peterson, Jay M Ver Hoef, Matthew C Groce, Dona L Horan, and David E Nagel. Slow climate velocities of mountain streams portend their role as refugia for cold-water biodiversity. *Proceedings of the National Academy of Sciences*, 113(16): 4374–4379, 2016.

Suzanne J Kelson and Stephanie M Carlson. Do precipitation extremes drive growth and migration timing of a pacific salmonid fish in mediterranean-climate streams? *Ecosphere*, 10(3):e02618, 2019.

Suzanne J Kelson, Stephanie M Carlson, and Michael R Miller. Indirect genetic control of migration in a salmonid fish. *Biology letters*, 16(8):20200299, 2020.

James W Kirchner. Catchments as simple dynamical systems: Catchment characterization, rainfall-runoff modeling, and doing hydrology backward. *Water Resources Research*, 45(2), 2009.

Axel Kleidon. Global datasets of rooting zone depth inferred from inverse methods. *Journal of Climate*, 17(13):2714–2722, 2004.

P Zion Klos, Michael L Goulden, Clifford S Riebe, Christina L Tague, A Toby O'Geen, Brady A Flinchum, Mohammad Safeeq, Martha H Conklin, Stephen C

Hart, Asmeret Asefaw Berhe, et al. Subsurface plant-accessible water in mountain ecosystems with a mediterranean climate. *Wiley Interdisciplinary Reviews: Water*, 5 (3):e1277, 2018.

Barret L Kurylyk, Kerry TB MacQuarrie, Daniel Caissie, and Jeffrey M McKenzie. Shallow groundwater thermal sensitivity to climate change and land cover disturbances: derivation of analytical expressions and implications for stream temperature modeling. *Hydrology and Earth System Sciences*, 19(5):2469–2489, 2015.

Theodore R Labbe and Kurt D Fausch. Dynamics of intermittent stream habitat regulate persistence of a threatened fish at multiple scales. *Ecological Applications*, 10(6):1774–1791, 2000.

Dana A Lapides, W. Jesse Hahm, Daniella Rempe, William E Dietrich, and David N Dralle. Controls on streamwater age in a saturation overland flow-dominated catchment. *Earth and Space Science Open Archive*, page 37, 2021. doi: 10.1002/essoar.10508976.1.

JA Leach and RD Moore. Observations and modeling of hillslope throughflow temperatures in a coastal forested catchment. *Water Resources Research*, 51(5):3770–3795, 2015.

Jason A Leach and Dan Moore. Insights on stream temperature processes through development of a coupled hydrologic and stream temperature model for forested coastal headwater catchments. *Hydrological Processes*, 31(18):3160–3177, 2017.

Jason A Leach and R Dan Moore. Empirical stream thermal sensitivities may underestimate stream temperature response to climate warming. *Water Resources Research*, 55(7):5453–5467, 2019.

Bernhard Lehner, Catherine Reidy Liermann, Carmen Revenga, Charles Vörösmarty, Balazs Fekete, Philippe Crouzet, Petra Döll, Marcel Endejan, Karen Frenken, Jun Magome, and et al. High-resolution mapping of the world's reservoirs and dams for sustainable river-flow management. *Frontiers in Ecology and the Environment*, 9(9):494–502, May 2011. ISSN 1540-9309. doi: 10.1890/100125. URL `http://dx.doi.org/10.1890/100125`.

Peter J Lisi, Daniel E Schindler, Kale T Bentley, and George R Pess. Association between geomorphic attributes of watersheds, water temperature, and salmon spawn timing in alaskan streams. *Geomorphology*, 185:78–86, 2013.

David G Litwin, Gregory E Tucker, Katherine R Barnhart, and Ciaran J Harman. Groundwater affects the geomorphic and hydrologic properties of coevolved landscapes. *Journal of Geophysical Research: Earth Surface*, page e2021JF006239, 2020.

S. M. Lovill, W. J. Hahm, and W.E. Dietrich. Drainage from the critical zone: Lithologic controls on the persistence and spatial extent of wetted channels during the summer dry season. *Water Resources Research*, 54(8):5702–5726, Aug 2018a. ISSN 1944-7973. doi: 10.1029/2017wr021903. URL `http://dx.doi.org/10.1029/2017WR021903`.

SM Lovill, WJ Hahm, and WE Dietrich. Drainage from the critical zone: lithologic controls on the persistence and spatial extent of wetted channels during the summer dry season. *Water Resources Research*, 54(8):5702–5726, 2018b.

Tessa Maurer, Francesco Avanzi, Steven D. Glaser, and Roger C. Bales. Drivers of drought-induced shifts in the water balance through a budyko approach. Mar 2021. doi: 10.5194/hess-2021-55. URL `http://dx.doi.org/10.5194/hess-2021-55`.

Erica L McCormick, David N Dralle, W Jesse Hahm, Alison K Tune, Logan M Schmidt, K Dana Chadwick, and Daniella M Rempe. Widespread woody plant use of water stored in bedrock. *Nature*, 597(7875):225–229, 2021.

JJ McDonnell, J Evaristo, KD Bladon, J Buttle, IF Creed, SF Dymond, Gordon Grant, A Iroume, CR Jackson, JA Jones, et al. Water sustainability and watershed storage. *Nature Sustainability*, 1(8):378–379, 2018.

Robert J McLaughlin, WV Sliter, NO Frederiksen, WP Harbert, and DS McCulloch. Plate motions recorded in tectonostratigraphic terranes of the franciscan complex and evolution of the mendocino triple junction, northwestern california. *US Geological Survey Bulletin*, 1997, 1994.

H Moidu, M Obedzinski, SM Carlson, and TE Grantham. Spatial patterns and sensitivity of intermittent stream drying to climate variability. *Water Resources Research*, 57(11):e2021WR030314, 2021.

David R Montgomery. Coevolution of the pacific salmon and pacific rim topography. *Geology*, 28(12):1107–1110, 2000.

David R Montgomery, Tamara M Massong, and Suzanne C S Hawley. Influence of debris flows and log jams on the location of pools and alluvial channel reaches, Oregon Coast Range. *Geological Society of America Bulletin*, page 11, 2003.

Marc F. Müller, David N. Dralle, and Sally E. Thompson. Analytical model for flow duration curves in seasonally dry climates. *Water Resources Research*, 50 (7):5510–5531, Jul 2014. ISSN 0043-1397. doi: 10.1002/2014wr015301. URL `http://dx.doi.org/10.1002/2014WR015301`.

Mariska Obedzinski, Sarah Nossaman Pierce, Gregg E Horton, and Mathew J Deitch. Effects of flow-related variables on oversummer survival of juvenile coho salmon in intermittent streams. *Transactions of the American Fisheries Society*, 147(3):588–605, 2018.

DJ Orth, CW Krause, and DC Novinger. Influences of fluctuating flows on spawning habitat and recruitment success. In *AGU Spring Meeting Abstracts*, volume 2005, pages B53B–02, 2005.

Michelle A. Pedrazas, W. Jesse Hahm, Mong-Han Huang, David Dralle, Mariel D. Nelson, Rachel E. Breunig, Kristen E. Fauria, Alexander B. Bryk, William E. Dietrich, and Daniella M. Rempe. The relationship between topography, bedrock weathering, and water storage across a sequence of ridges and valleys. *Journal* *of Geophysical Research: Earth Surface*, 126(4), Apr 2021. ISSN 2169-9011. doi: 10.1029/2020jf005848. URL `http://dx.doi.org/10.1029/2020JF005848`.

Jon D Pelletier, Patrick D Broxton, Pieter Hazenberg, Xubin Zeng, Peter A Troch, Guo-Yue Niu, Zachary Williams, Michael A Brunke, and David Gochis. A gridded global data set of soil, intact regolith, and sedimentary deposit thicknesses for regional and global land surface modeling. *Journal of Advances in Modeling Earth Systems*, 8(1): 41–65, 2016.

Jonathan Perkins. South Fork Eel River, CA: Understanding Terrace Formation and Abandonment. 2009. doi: 10.5069/G93F4MH1.

Mary E. Power. South Fork Eel River, CA Watershed Morphology. 2013. doi: 10.5069/G9639MPN.

Jeff P Prancevic and James W Kirchner. Topographic controls on the extension and retraction of flowing streams. *Geophysical Research Letters*, 46(4):2084–2092, 2019.

PRISM Climate Group. Prism rainfall dataset. 2004. URL `http://prism.oregonstate.edu`.

Thomas P Quinn, Sayre Hodgson, and Charles Peven. Temperature, flow, and the migration of adult sockeye salmon (oncorhynchus nerka) in the columbia river. *Canadian Journal of Fisheries and Aquatic Sciences*, 54(6):1349–1360, Jun 1997. ISSN 1205-7533. doi: 10.1139/f97-038. URL `http://dx.doi.org/10.1139/f97-038`.

Daniella M Rempe and William E Dietrich. A bottom-up control on fresh-bedrock topography under landscapes. *Proceedings of the National Academy of Sciences*, 111 (18):6576–6581, 2014.

Daniella M. Rempe and William E. Dietrich. Direct observations of rock moisture, a hidden component of the hydrologic cycle. *Proceedings of the National Academy of Sciences*, 115(11):2664–2669, Feb 2018. ISSN 1091-6490. doi: 10.1073/pnas.1800141115. URL `http://dx.doi.org/10.1073/pnas.1800141115`.

Clifford S. Riebe, W. Jesse Hahm, and Susan L. Brantley. Controls on deep critical zone architecture: a historical review and four testable hypotheses. *Earth Surface Processes and Landforms*, 42(1):128–156, Nov 2016. ISSN 0197-9337. doi: 10.1002/esp.4052. URL `http://dx.doi.org/10.1002/esp.4052`.

Josh Roering. Eel River, CA: Landsliding and the Evolution of Mountainous Landscapes. 2006. doi: 10.5069/G9XS5S9P.

Joshua J Roering, Benjamin H Mackey, Alexander L Handwerger, Adam M Booth, David A Schmidt, Georgina L Bennett, and Corina Cerovski-Darriau. Beyond the angle of repose: A review and synthesis of landslide processes in response to rapid uplift, eel river, northern california. *Geomorphology*, 236:109–131, 2015.

Gabriel Jacob Rossi. *Food, Phenology, and Flow: How Prey Phenology and Streamflow Dynamics Affect the Behavior, Ecology, and Recovery of Pacific Salmon.* University of California, Berkeley, 2020.

G.J. Rossi, M.E. Power, S. M. Carlson, and T.E. Grantham. Seasonal growth potential of oncorhynchus mykiss in streams with contrasting prey phenology and streamflow. *Ecosphere*, 2022.

John L Sabo, Jacques C Finlay, Theodore Kennedy, and David M Post. The role of discharge variation in scaling of drainage area and food chain length in rivers. *science*, 330(6006):965–967, 2010.

Rohit Salve, Daniella M Rempe, and William E Dietrich. Rain, rock moisture dynamics, and the rapid response of perched groundwater in weathered, fractured argillite underlying a steep hillslope. *Water Resources Research*, 48(11), 2012.

Takahiro Sayama, Jeffrey J. McDonnell, Amod Dhakal, and Kate Sullivan. How much water can a watershed store? *Hydrological Processes*, 25(25):3899–3908, Oct 2011. ISSN 0885-6087. doi: 10.1002/hyp.8288. URL http://dx.doi.org/10.1002/hyp.8288.

H Jochen Schenk. The shallowest possible water extraction profile: a null model for global root distributions. *Vadose Zone Journal*, 7(3):1119–1124, 2008.

Daniel E Schindler, Ray Hilborn, Brandon Chasco, Christopher P Boatright, Thomas P Quinn, Lauren A Rogers, and Michael S Webster. Population diversity and the portfolio effect in an exploited species. *Nature*, 465(7298):609–612, 2010.

Logan Schmidt and Daniella Rempe. Quantifying dynamic water storage in unsaturated bedrock with borehole nuclear magnetic resonance. *Geophysical Research Letters*, 47 (22):e2020GL089600, 2020.

Leo Shapovalov and Alan C Taft. *The life histories of the steelhead rainbow trout (Salmo gairdneri gairdneri) and silver salmon (Oncorhynchus kisutch) with special reference to Waddell Creek, California, and recommendations regarding their management*, volume 98. Department of Fish and Game, State of California, 1954.

Chris Soulsby, Christian Birkel, and Doerthe Tetzlaff. Modelling storage-driven connectivity between landscapes and riverscapes: Towards a simple framework for long-term ecohydrological assessment. *Hydrological Processes*, 30(14):2482–2497, 2016.

J St. Clair, S Moon, WS Holbrook, JT Perron, CS Riebe, SJ Martel, B Carr, C Harman, d Singha, K, and D deB Richter. Geophysical imaging reveals topographic stress control of bedrock weathering. *Science*, 350(6260):534–538, 2015.

Maria Staudinger, Michael Stoelzle, Stefan Seeger, Jan Seibert, Markus Weiler, and Kerstin Stahl. Catchment water storage variation with elevation. *Hydrological Processes*, 31(11):2000–2015, Apr 2017. ISSN 0885-6087. doi: 10.1002/hyp.11158. URL http://dx.doi.org/10.1002/hyp.11158.

Benjamin D. Stocker, Shersingh Joseph Tumber-Dávila, Alexandra G. Konings, Martha B. Anderson, Christopher Hain, and Robert B. Jackson. Global distribution of the rooting zone water storage capacity reflects plant adaptation to the environment.

bioRxiv, 2021. doi: 10.1101/2021.09.17.460332. URL `https://www.biorxiv.org/content/early/2021/10/04/2021.09.17.460332`.

Maya F Stokes and J Taylor Perron. Modeling the evolution of aquatic organisms in dynamic river basins. *Journal of Geophysical Research: Earth Surface*, 125(9): e2020JF005652, 2020.

Anna M. Sturrock, Stephanie M. Carlson, John D. Wikert, Tim Heyne, Sébastien Nusslé, Joseph E. Merz, Hugh J. W. Sturrock, and Rachel C. Johnson. Unnatural selection of salmon life histories in a modified riverscape. *Global Change Biology*, 26(3):1235–1247, Dec 2019. ISSN 1365-2486. doi: 10.1111/gcb.14896. URL `http://dx.doi.org/10.1111/gcb.14896`.

Gregory E. Sykes, Chris J. Johnson, and J. Mark Shrimpton. Temperature and flow effects on migration timing of chinook salmon smolts. *Transactions of the American Fisheries Society*, 138(6):1252–1265, Nov 2009. ISSN 1548-8659. doi: 10.1577/t08-180.1. URL `http://dx.doi.org/10.1577/T08-180.1`.

M.M. Thornton, R. Shrestha, Y. Wei, P.E. Thornton, S. Kao, and B.E. Wilson. Daymet: Daily surface weather data on a 1-km grid for north america, version 4, 2020.

Alison K Tune, Jennifer L Druhan, Jia Wang, Philip C Bennett, and Daniella M Rempe. Carbon dioxide production in bedrock beneath soils substantially contributes to forest carbon cycling. *Journal of Geophysical Research: Biogeosciences*, 125(12): e2020JG005795, 2020.

Pedro Val, Nathan J Lyons, Nicole Gasparini, Jane K Willenbring, and James S Albert. Landscape evolution as a diversification driver in freshwater fishes. *Frontiers in Ecology and Evolution*, page 975, 2022.

Ross Vander Vorste, Mariska Obedzinski, Sarah Nossaman Pierce, Stephanie M Carlson, and Theodore E Grantham. Refuges and ecological traps: Extreme drought threatens persistence of an endangered fish in intermittent streams. *Global change biology*, 26 (7):3834–3845, 2020.

Jonathan A Wald, Robert C Graham, and Phillip J Schoeneberger. Distribution and properties of soft weathered bedrock at less than 1 m depth in the contiguous united states. *Earth Surface Processes and Landforms*, 38(6):614–626, 2013.

Lan Wang-Erlandsson, Wim GM Bastiaanssen, Hongkai Gao, Jonas Jägermeyr, Gabriel B Senay, Albert IJM Van Dijk, Juan P Guerschman, Patrick W Keys, Line J Gordon, and Hubert HG Savenije. Global root zone storage capacity from satellite-based evaporation. *Hydrology and Earth System Sciences*, 20(4):1459–1481, 2016.

Robin S Waples, George R Pess, and Tim Beechie. Evolutionary history of pacific salmon in dynamic environments. *Evolutionary Applications*, 1(2):189–206, 2008.

Bruce W Webb, David M Hannah, R Dan Moore, Lee E Brown, and Franz Nobilis. Recent advances in stream and river temperature research. *Hydrological Processes: An International Journal*, 22(7):902–918, 2008.

Cleo Woelfle-Erskine, Laurel G Larsen, and Stephanie M Carlson. Abiotic habitat thresholds for salmonid over-summer survival in intermittent streams. *Ecosphere*, 8 (2):e01645, 2017.

Sarah M Yarnell, Eric D Stein, J Angus Webb, Theodore Grantham, Rob A Lusardi, Julie Zimmerman, Ryan A Peek, Belize A Lane, Jeanette Howard, and Samuel Sandoval-Solis. A functional flows approach to selecting ecologically relevant flow metrics for environmental flow applications. *River Research and Applications*, 36(2): 318–324, 2020.

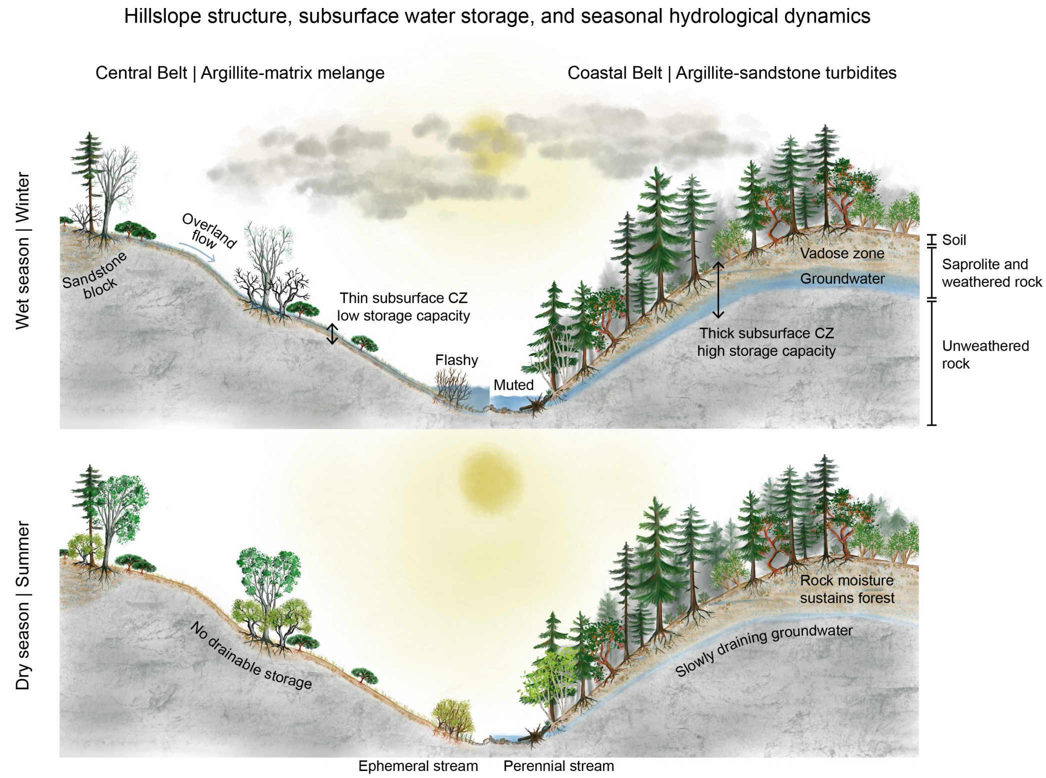

Figure 1. Seasonal hydrological dynamics between hillslopes representing two dominant geologies in the Eel River watershed — Central Belt mélange (left) and Coastal Belt turbidites (right) — leading to contrasting CZ architectures and water storage capacities. A typical wet season (winter) snapshot is depicted in the top row, while the bottom row illustrates conditions later in the dry season (summer).

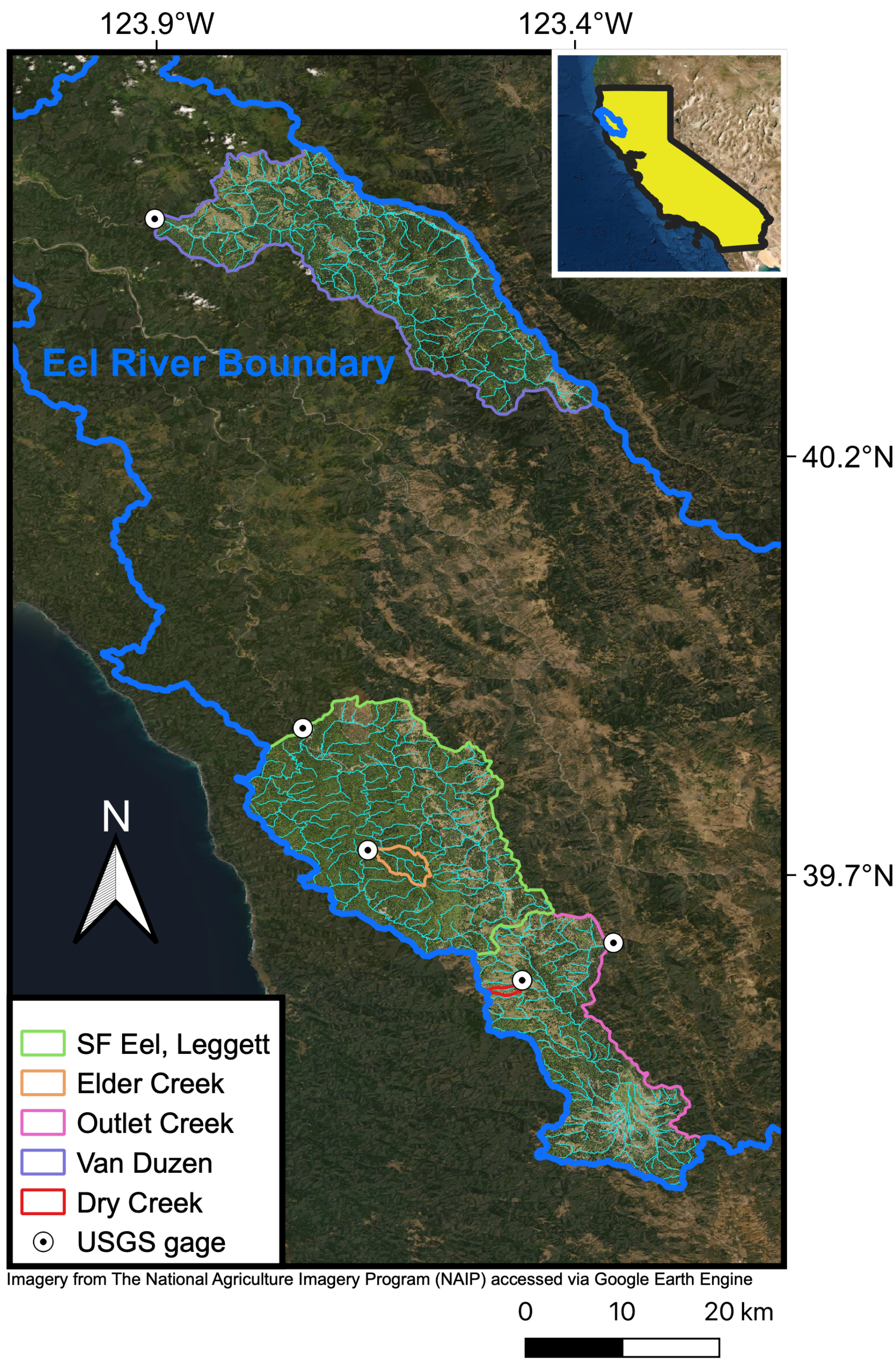

Figure 2. Overview map of the study watersheds.

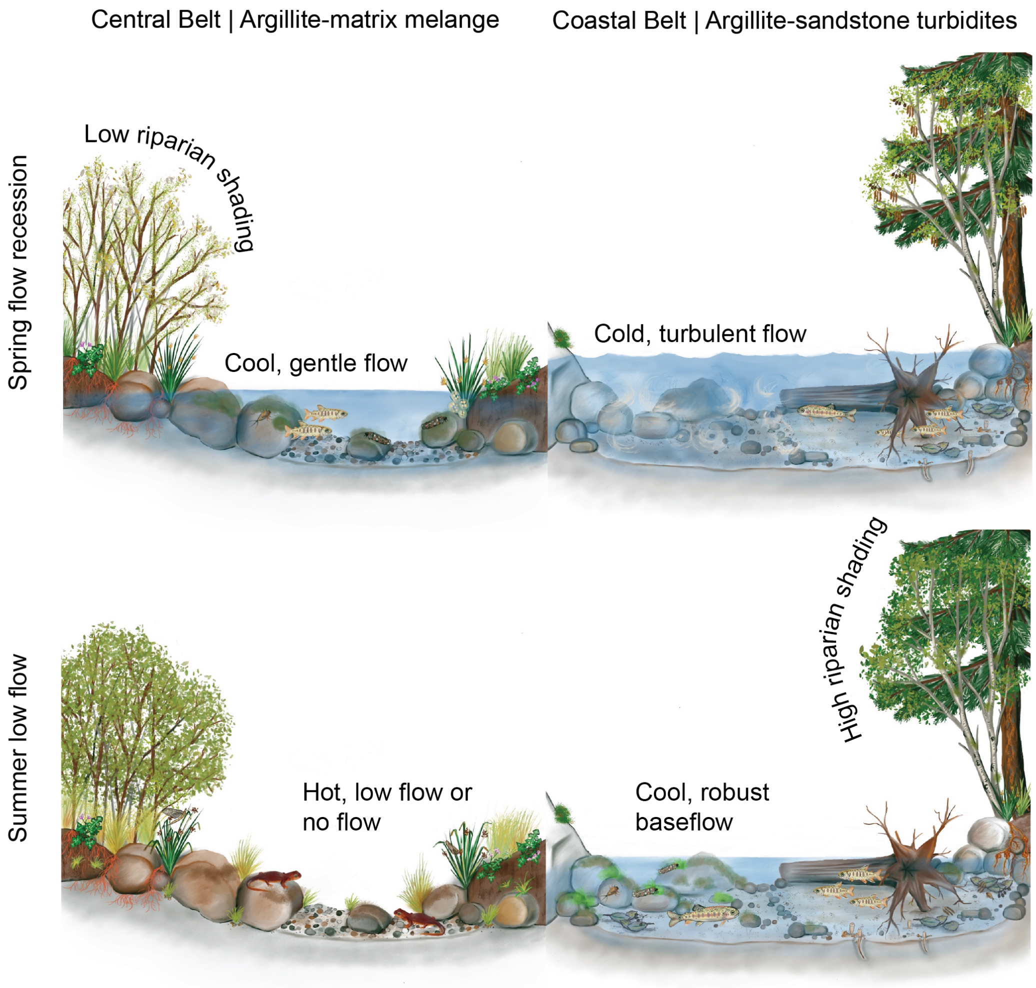

Figure 3. Typical progression of stream conditions between the Central Belt mélange (left) and Coastal Belt turbidites (right) following the last significant rainfall event of the wet season. The top row illustrates conditions in the spring/early summer when air temperatures have begun to increase and stream flow is beginning its long seasonal recession. The bottom row depicts late summer low flow conditions when air temperatures are high and water availability in the stream is approaching its annual minimum.

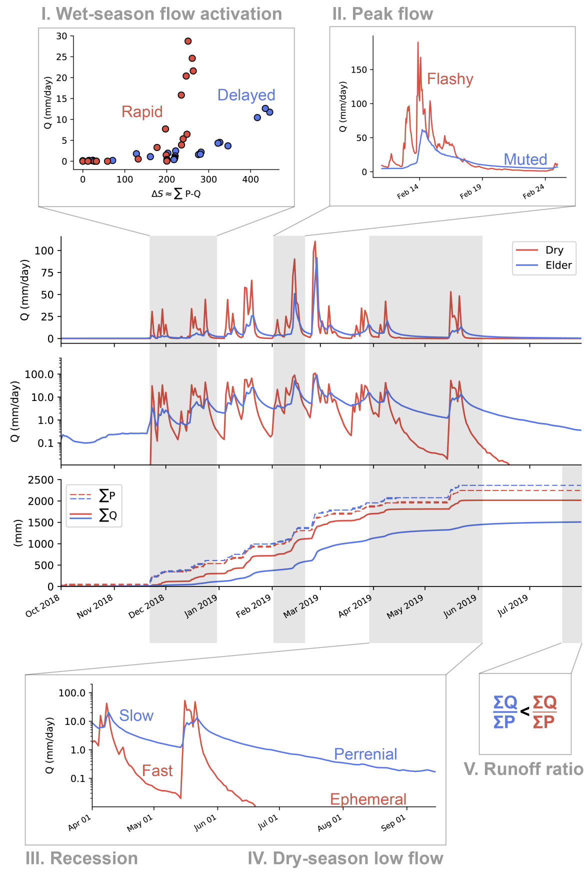

Figure 4. Storage capacity impacts important flow regime characteristics. Roman numerals correspond to entries in Table 2, while blue and red colors correspond to the Elder Creek and Dry Creek watersheds, which are representative end members of the Coastal Belt (relatively high storage capacity) and mélange (low storage capacity) geologies, respectively. The top two subplots of the center panel show 2019 water year hydrographs (on linear and log scales), while the bottom subplot shows cumulative precipitation ($\sum P$) and cumulative discharge ($\sum Q$). Focus panel (I) plots initial wet-season discharge as a function of the approximate dynamic storage $\sum P - Q$. (II) shows an expanded view of peak flows during a typical wet season storm sequence after initial wet-up. (III) illustrates differences in recession rates, while (IV) demonstrates how recession rate determines whether or not streams continue to flow through the entire dry season. (V) shows that a greater fraction of precipitation is converted to runoff in the Dry Creek watershed.

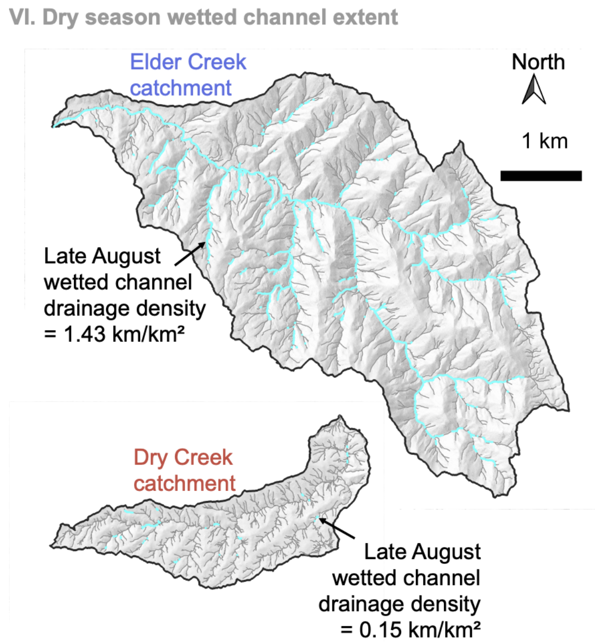

Figure 5. Dry season wetted channel extent is approximately tenfold higher in the representative Coastal belt watershed (Elder Creek) than the representative Central belt watershed (Dry Creek). Cyan lines denote liquid water at surface in channels (including all stagnant pools and flowing reaches, whether disconnected or continuous). Light grey lines denote approximate geomorphic channel extent. Each catchment is shown to scale but their relative locations have been modified for display purposes. Wetted channel data from Lovill et al. [2018b]; Elder Creek surveyed in 2014, Dry Creek in 2015. LiDAR-derived hillshade underlays from data collected by NCALM [Dietrich, 2014].

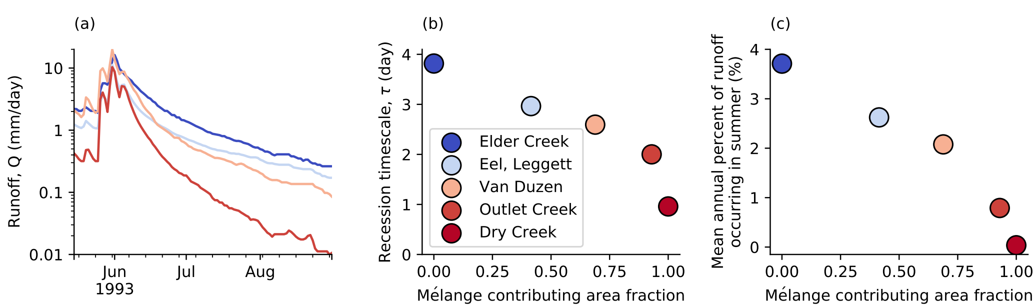

Figure 6. Watersheds across a gradient in fraction of mélange contributing area illustrate a range of flow recession behaviors (left subplot). The five colored points refer to the watersheds described in Table 3. Recession analysis (middle subplot) shows that larger fractional mélange contributing area results in faster recessions, as quantified by a simple exponential recession model: $Q(t) = Q_0 e^{-t/\tau}$. Smaller values of τ in mélange-dominated watersheds correspond correspond to faster recessions (i.e. rapid timescales of drainage). One consequence of the fast mélange recession is decreased water availability during the dry season, as demonstrated by the decrease in summer runoff fraction with increasing mélange fraction (right subplot). Conversely, Coastal Belt watersheds drain much more slowly, resulting in perennial flows and robust dry season discharge.

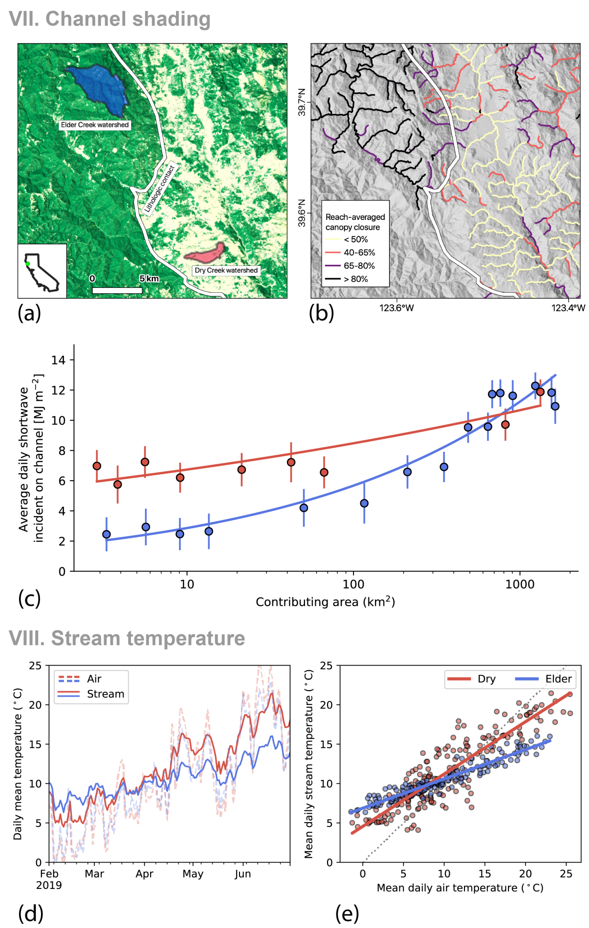

Figure 7. Differences in storage capacity across the geologic contact lead to stark differences in vegetation cover (a). Representative end-member catchments are outlined. Differences in canopy cover result in smaller delivery of shortwave radiation to headwater channel surfaces during summer months (June, July, August) in the Coastal belt (west of contact) versus Central belt (east of contact) (b). With increasing contributing area, channels widen, resulting in a convergence of channel-incident shortwave radiation between the two geologies (c). Red and blue points are binned averages ± one standard deviation, from all Central belt and Coastal belt channels, respectively, in study area with available LiDAR data. Bin spacing varies to ensure a sufficient number of samples in each bin according to the procedure described in Kirchner [2009]. Contrasting stream temperature dynamics (d) due to differences in flow pathways, flow volumes, and riparian light environment. Subplot (e) demonstrates significantly higher sensitivity to changes in air temperature in the Dry Creek watershed.

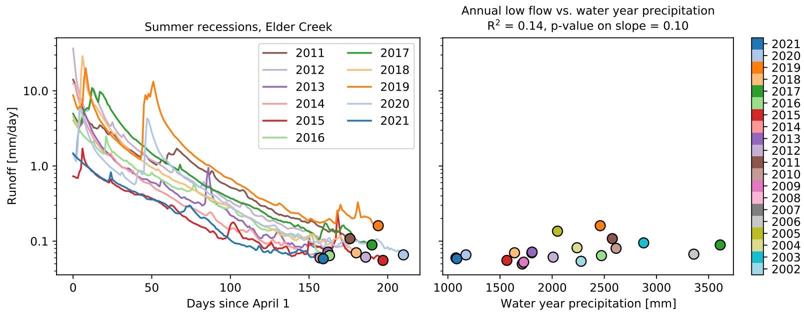

Figure 8. Storage capacity decouples annual low flows from *total* water year precipitation at Elder Creek. (a) plots summer recessions as a function of days after April 1 from 2011 water year through 2021 water year, stopping on the day with the lowest observed flow for that calendar year (through December). The second subplot (b) shows that annual total precipitation is not a strong predictor of dry season low flows due to the mechanism of storage-capacity limitation. End-of-dry-season low flow conditions are more strongly controlled by rainfall conditions during the transition between wet and dry seasons. Annual rainfall data is derived from the PRISM Climate Group [PRISM Climate Group, 2004] daily rainfall product found on the Google Earth Engine Data Catalog.

GLOSSARY

Term/quantity	**Definition**	**Dimensions**
Dynamic storage (ΔS)	The volume of water stored in a catchment relative to some reference storage state, commonly taken to be zero at the driest time of year.	[L] or [L^3]
Storage capacity	The maximum observed value of dynamic storage.	[L] or [L^3]
Runoff (Q)	Stream discharge. Expressed in volumetric units (e.g. cubic meters per second), but also commonly reported in area-normalized units (e.g. mm/day) to facilitate runoff production intercomparisons between watersheds with different areas.	[L/T] or [L^3/T]
Evapotranspiration (ET)	The sum of water use by vegetation (transpiration) and water returned to the atmosphere via evaporative losses from the ground surface or water bodies.	[L/T]
Recession timescale (τ)	Determines the flow recession rate under the assumption that Q decline is linearly proportional to Q (i.e. $dQ/dt = -\frac{1}{\tau}Q$), leading to an exponential functional form for the streamflow recession.	[T]
Light penetration index (LPI)	The number of LiDAR returns from the ground or water surface divided by the total number of LiDAR returns.	Unitless
Runoff ratio	The ratio of total stream discharge to total precipitation over some time interval. Typically expressed over annual or longer timescales.	Unitless
Drainage density	The length of stream channel per area of watershed.	[L^{-1}]
Saturation overland flow	Overland flow that occurs when groundwater tables rise from below and intersect the ground surface, leading to runoff production via direct precipitation on saturated areas or water exfiltrating from the groundwater (return flow).	[L/T] or [L^3/T]
Contributing area	Defined at a point, the total upstream watershed area draining all streams and hillslopes to that point.	[L^2]

Table 1. Table of terminology

Observed impacts of hillslope subsurface water storage capacity on streamflow characteristics in rain-dominated, Mediterranean climates

Category	Metric	Relative impact	Hypothesized reason/mechanism
Water	I. Wet season flow activation	Later with bigger storage capacity	More rain required to replenish bigger dry season hillslope water storage deficits
	II. Peakflow magnitude	Higher with smaller storage capacity	Small storage capacity more likely to fill, prompting greater and activation of faster (shallow near surface or overland) runoff pathways
	III. Rate of recession	Higher with smaller storage capacity	Deep slow flowpaths versus shallow fast flowpaths
	IV. Mean low (base)flow magnitude	Higher with bigger storage capacity	Greater reservoir to sustain dry season flow
	V. Annual runoff ratio	Lower with bigger storage capacity	More rainfall is partitioned to evapotranspiration where storage capacity is greater, enabling storage of wet-season rainfall for dry-season use by plants
	VI. Dry season wetted channel extent	Lower with smaller storage capacity	Lower supply of flow from hillslopes to channels
Energy	VII. Stream temperature	Colder in winter and warmer in summer with smaller storage capacity	Small storage capacity promotes shallower hillslope runoff pathways through regions similar to ambient air temperature; big storage capacity promotes deep hillslope runoff pathways through regions with mean annual air temperature
	VIII. Channel shading	Lower with smaller storage capacity in headwaters	Small storage capacity limit growth of plants, decreasing shade adjacent to channel; at large areas channel is sufficiently wide that riparian vegetation shading becomes less important

Table 2. Observed impacts of hillslope subsurface water storage capacity on streamflow characteristics in rain-dominated, Mediterranean climates

Watershed	**USGS gage ID**	**Area (km2)**	**Mapped % mélange geology***
Dry Creek	N/A	3.5	100%
Outlet Creek	11472200	418	92%
Van Duzen River	11478500	574	68%
Eel River, Leggett	11475800	642	41%
Elder Creek, Branscomb	11475560	16.8	0%

Table 3. * Non-mélange geology for these watersheds is predominantly Coastal Belt, with the exception of the Van Duzen River which also includes portions of the Eastern Belt.